



Development of a miniature low-temperature solar seawater desalination device

Zetian Mao^{a,1}, Yan Chen^{b,1}, Jie Ren^c, Chunsheng Guo^{a,*}, Hai Liu^a, Jun Gao^a

^aSchool of Mechanical, Electronic & Engineering, Shandong University at Weihai, 264209 Weihai, China, Tel. +86-13573728778; email: guo@sdu.edu.cn (C.S. Guo), Tel. +86-13296302076; email: zetian_mao@outlook.com (Z. Mao), Tel. +86-13863117601; email: sdulh8691@163.com (H. Liu), Tel. +86-15263120055; email: shdgj@sdu.edu.cn (J. Gao)

^bSchool of Energy and Power Engineering, Shandong University, Jinan 250061, China, Tel. +86-15954102000; email: henyang79@sdu.edu.cn (Y. Chen)

^cSchool of Space Science and Physics, Shandong University at Weihai, 264209 Weihai, China, Tel. +86-13304731050; email: rallor@foxmail.com

Received 9 October 2018; Accepted 7 July 2019

ABSTRACT

Traditional seawater desalination is an energy-intensive industry and desalination with new clean renewable energy sources will become an important developing direction. Especially on ships and in areas where there are serious fresh water or power shortage problems, the implement of seawater desalination with solar energy is of far-reaching practical significance. Based on the enhanced heat transfer mechanism of the horizontal tube falling film evaporator, and the internal and external fin tube condenser, a set of miniature low-temperature single-effect solar seawater desalination device was developed. The designed parameters of the main heat transfer elements of the seawater desalination system were obtained by mathematical simulation and the simulation experiment was carried out by the simulated solar energy using electric heating tank. In the experiment, the transient and steady-state performance of the system is tested. The water producing rate, coefficients of the falling film horizontal tube performance and coefficients of the condensing pipe performance under different flow and temperature conditions are given, which provides an effective method for the design of the miniature low-temperature solar desalination device. The results show that the system has a high water producing rate and fresh water output efficiency under steady-state conditions through a series of enhanced heat transfer measures. At present, the water producing rate can reach 1.6 L/h when the heating water temperature is 75°C–85°C, and the stable water producing rate can reach 8 L/h. Relevant experimental data provide data support for the design of small desalination plants.

Keywords: Seawater desalination; Low-temperature; Solar distillation; Transient and steady-state experiments

1. Introduction

Fresh water is the key natural resource for human survival and development. Since the 20th century, the requirement of fresh water has been increasing drastically due to the explosive growth of population and the development of industry.

It is discovered that 71% of the earth surface is covered by water. However, only 3% is presented as portable water and only 1% is accessible to human beings [1]. It is predicted that close to 70% of the world population will be threatened by the water-shortage problem and approximately 50% of the world's population lives within 200 km of the coast [2].

* Corresponding author.

¹ These two authors contributed equally to this study and share the first authorship.

Due to the geographical coincidence between water shortage and high solar irradiance, solar energy has the highest potential for water desalination applications [1]. The present seawater desalination market has been dominated by three processes of thermal evaporation, reverse osmosis and electro-dialysis (ED) [3–9]. However, these technologies need high power consumption and are unsuitable for remote villages and small islands because of power supply problems and limited space. Therefore, the study and development of a miniature low-temperature solar seawater desalination device is of great significance.

The thermal type seawater desalination is a very simple process because the pure freshwater is obtained by condensing the steam after evaporating seawater [10]. The distillation seawater desalination is one of the thermal evaporation methods, which currently refers to a low-temperature distillation seawater desalination method. Low-temperature distillation means that the top brine temperature does not exceed 70°C. Fouling and corrosion are known to escalate at high solution temperatures and the threshold for high salt deposition from the saline solution is known to occur when temperatures exceed 80°C [11]. When the temperature is below 70°C, due to the lower temperature, the salt deposition rate on the metal evaporator surface largely decrease, which can significantly reduce seawater corrosion [12]. This technology has the advantages of low operating temperature and minimal seawater reserves in the device (the device starts up fast) [13] and is easy to be combined with solar-heating systems. The energy-saving factor is developing rapidly, the device scale is expanding, and the cost is declining.

Active solar distillation seawater desalination equipment has developed rapidly in recent years. It overcomes the shortcomings of passive solar distillation systems. Tiwari and Sahota [14] reviewed the research on passive and active solar distillation in detail. They also provided further research targets and suggestions about solar stills for sustainable potable water production. Tiwari et al. [15] presented exergoeconomic and enviroeconomic analyses of a partially covered photovoltaic thermal (PVT) flat plate collector (FPC)-integrated solar distillation system known as PVT-FPC active solar distillation system. The performance had been valued and compared with earlier researches. Reddy and Sharon [16] proposed an active multistage series solar distillation and its performance, environmental benefits and economic feasibility were assessed by conducting 3E (energy–environment–economic) analyses using a developed mathematical model. Chandrashekhara and Avadhesh [17] presented an overall review and a technical assessment of various and up-to-date developments in single and multi-effect solar stills. The problem of unit development and the impact on the environment were solved during the development and operation of static configuration. El-Sebaii and El-Bialy [18] reviewed the works on solar distillation, its present status in the world and its future perspective. The review also included water sources, water demand, availability of potable water, and purification methods. Srikantha [19] designed and developed an active vacuum distillation solar water purification device. This device has attracted considerable attention and increased the possibility of autonomous construction of the system in rural areas through low costs. Ithape et al. [20] analyzed the effects of different parameters on the performance

of a solar distillation system, and Hansen and Murugavel [21] conducted experimental studies on a new hybrid solar desalination system on different novel absorber structures.

The designed simulation of the distilling seawater desalination device in the aforementioned literature is quite different from the actual working conditions. For example, the system thermodynamic model does not study the influencing factors of water production. In the scope of research in distillation field, steam is taken as a heat source in some thermodynamic models, but steam is currently used in multi-effect and large-scale distilled seawater desalination plants. Only few desalination technologies refer to small-scale thermal desalination plants.

Siddique et al. [22] did a comparative analysis for small-scale low pressure ‘single-effect distillation’ and ‘single-stage flash’ solar-driven barometric desalination units. They concluded that the solar-driven barometric SED type units have a considerably better performance over the SSF type units in all comparison aspects including heat input rate, seawater feed rate and costs. So this article selected SED type to develop a small-scale low-temperature solar distillation seawater desalination device based on the enhanced heat transfer mechanism of horizontal-tube falling-film evaporation and internal and external fin tubes condensation. Solar energy is utilized as a heat source. Compared with fossil fuel energy source, solar energy has the advantages of safety and environmental protection. Combining the two systems of solar energy collection and distillation process is a sustainable seawater desalination technology. A heat transfer experimental platform was built. A pipe heater was used to simulate solar energy as hot water input and an industrial chiller was used to simulate cold water input. Transient and steady-state experiments were performed on the system. In the experiment, the heat transfer component’s data of temperature difference and output were recorded with flow rate and water temperature variance in the horizontal tube falling film evaporator, the internal and external fin condenser tubes and temperature. The experimental relation between various parameters and water producing performance is given.

2. Introduction to the miniature solar low-temperature distillation seawater desalination system

The miniature low-temperature solar desalination device is composed of a main evaporation chamber and peripheral pipelines. The evaporation chamber mainly includes a horizontal-tube falling-film evaporator, an internal and external fin condenser, an atomizing spray, and freshwater collectors. The peripheral pipelines mainly include a simulated solar-heating electric heater, a simulated cooling source, a circulating spray pipe, solenoid valves, automatic control components, and connecting pipelines. The operating principle of the device can be described as follows.

The miniature low-temperature solar desalination device mainly adopts the following enhanced heat transfer process: horizontal cross-tube falling-film evaporation, convection heat transfer in the horizontal tube, internal and external fin condensation, convection heat transfer in the tube and so on. These processes make the miniature seawater desalination system have a high heat transfer performance. The simulated solar electric heating hot water outlet is connected

to the inlet of falling-film horizontal tube in the evaporation chamber tank. The energy released by hot water in the falling-film horizontal tube goes through the tube wall and evaporates the liquid film on the outer wall of the horizontal pipe. The hot steam rises to release heat and condenses at the internal and external fin condenser tube to generate fresh water. The fresh water drops into the freshwater storage via a freshwater collection line. When the freshwater volume reaches the set point, the valve connecting to the evaporation chamber is closed and the valve at ventage is opened to allow the fresh water to flow out.

In Fig. 1, ball valve: 1, 2, 3, 4, 5, 6, 7, 8; filter: 9, 10, 11; one-way pump: 12, 13, 14; thermocouple: 15, 16, 17, 18, 19; flowmeter: 20, 21, 22; one-way valve: 23; liquid level meter: 24; pressure meter: 25, 26; seawater for cooling circulation: 27; pretreated seawater: 28; solar collector: 29; freshwater collector: 30; spray: 31; condenser tube: 32; vacuum pump: 33; freshwater storage tank: 34.

The vacuum degree required by the system is provided by the vacuum pump. All principal components are wrapped with asbestos cloth to restrain heat transfer with the environment. After one-time spray is completed, circulating spray starts. The circulating spray pump presses the seawater in the tank towards the atomizing spray head. The sprayed seawater evaporates on the surface of horizontal pipes. The circulating process continues until the salinity of circulating water exceeds 100 g/kg. Then waste brine is drained and new feed water is ejected into the tank to start a new circle. The photo of desalination plant is shown in Fig. 2 and energy direction is shown in Fig. 3.

2.1. Horizontal-tube falling-film evaporator

Due to several advantages such as heat transfer with small temperature difference, suiting low-temperature evaporation,

high heat transfer coefficient and so on, horizontal tube evaporating technology has been the main technology in low-temperature desalination technology. In this system, the horizontal tube is arranged with several layers and two adjacent layers are cross-arranged. Such horizontal tube distribution makes seawater be sprayed evenly on each horizontal tube surface from the spray head above. Seawater and the working fluid in tubes can lead to a greater level of heat transfer.

The length, width and height of the evaporator are 20 cm, respectively. The vertical space between the two adjacent layers is 22.5 mm. The center distance of the two adjacent horizontal tubes in the same layer is 25 mm. The horizontal tube is manufactured with copper and its inner diameter is 8 mm with 2 mm wall thickness. The four vertical square walls are 304 stainless steel plates with 2 mm thickness. The 3D model and physical drawings are shown in Fig. 4.

2.2. Internal and external fin condenser tubes

The condenser adopts a new type of internal and external fin tube with a high heat transfer coefficient, in which the material is copper–nickel alloy. After annealing, the condenser is manufactured with a hob and has excellent corrosion resistance performance. Its main parameters are as follows: fin thickness $\delta_f = 0.35$ mm, fin spacing $S_f = 0.73$ mm, fin height $H_f = 1.8$ mm, fin tube inner minimum diameter $d_i = 14.6$ mm, and fin tube outer maximum diameter $d_o = 18.25$ mm, as shown in Fig. 5.

2.3. Atomized spray device

The bottom of the atomizing sprayer consists of four atomizing spray heads, and the spray heads are evenly distributed circularly. When the spray heads are under the

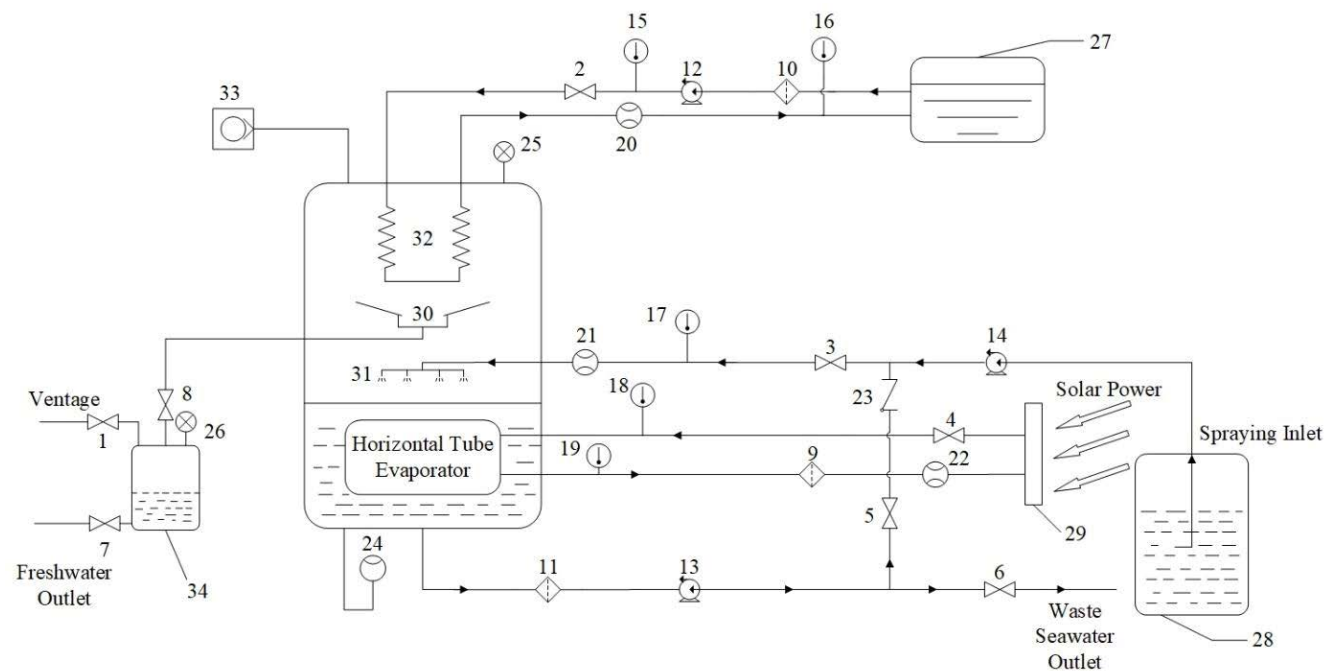


Fig. 1. Schematic of the low-temperature solar desalination system.



Fig. 2. Miniature low-temperature solar desalination setup.

pressure of 0.4 MPa, the atomized particle diameter is refined to 65 μm . The particles in this size form a water film layer on the evaporator. Spray heads made by acid-proof material can quantitatively spray sea water under the control of flow valve.

As shown in Fig. 6, the spray device is used in combination with the falling-film horizontal tube evaporator. The head pressure of sprayer is approximately 0.4 Mpa with an adjustable flow rate range of 0.3–1.5 L/min.

2.4. System control process

Upper computer program is software control platform programmed by C#. PC starts serial communication with controller (STM32) after clicking start button in the upper computer program. Serial communication is based on RS485

bus. The pin output of STM32 is connected to signal level converting module to control electric relay module. The program actuates electric relay to open upper node valve and start pump. All solenoid valves are supplied with 12 V and all pumps are supplied with 24 V. Then the device starts operation. Meanwhile, the voltage signal of the temperature, flow and pressure of each node is produced by thermal couple sensors, Hall flow sensors and pressure transmitter, respectively. The voltage signals are read into data collector by analog-digital conversion module and then upload to PC to plot graphs via serial communication.

3. Steady-state mathematical model of a miniature low-temperature distillation seawater desalination system

In this study, the low-temperature distillation seawater desalination system is taken as the research object, and a steady-state mathematical model is established, which includes the material and energy balance of the system. The above-mentioned balance is conducive to understanding the system material–energy relationship. The mathematical model can be used to calculate the expression of heat transfer coefficient at transverse tube and condenser pipe. The following assumptions are made to simplify the system model:

- The produced water vapor is pure water (namely the salinity of the water vapor is 0).
- Other gases except water vapor are non-condensable.
- The property of water both in liquid phase and gas phase is homogeneous, respectively.
- The system operates at relatively low temperatures, and the tank has good thermal insulation properties; therefore, the heat loss between the system and the environment is neglected.
- In the water temperature changing process, the latent heat of vaporization and the specific heat capacity of water did

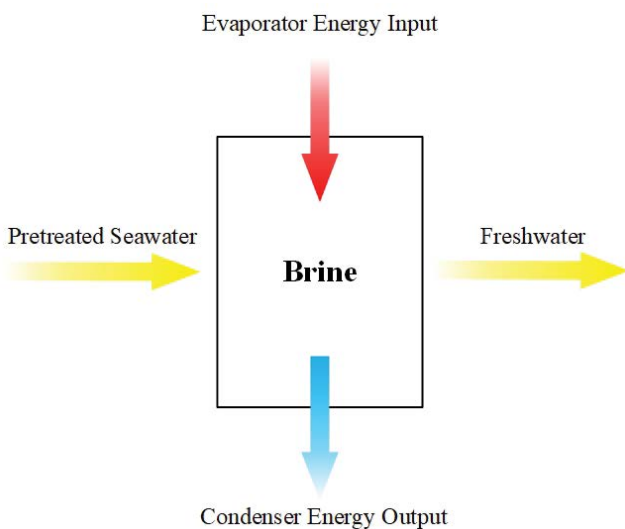


Fig. 3. Water balance diagram.



Fig. 4. Horizontal tube falling film evaporator.

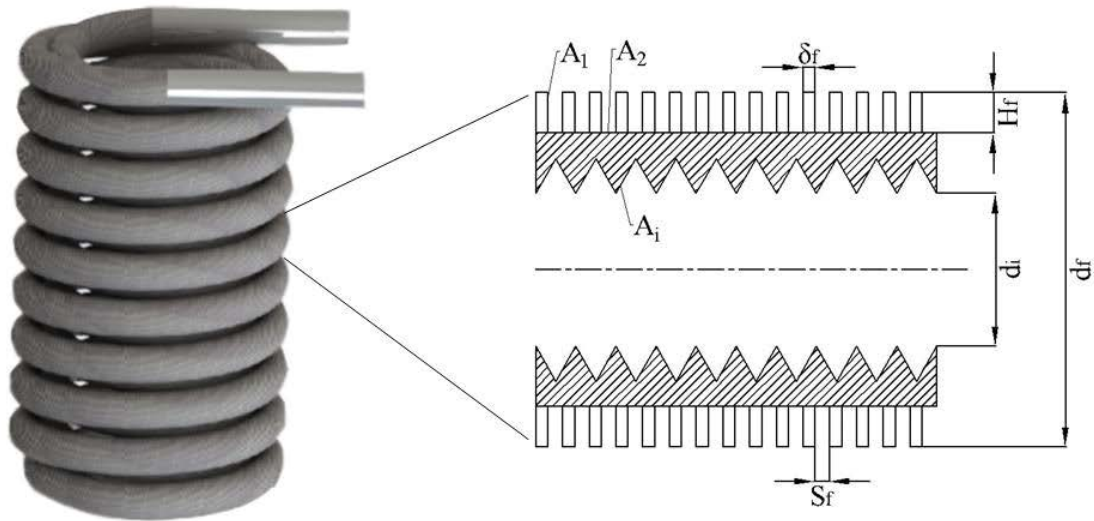


Fig. 5. Internal and external fin condensing tube.



Fig. 6. Atomizing spray device.

not change much in this paper, so the latent heat and specific heat capacity of water are taken as the constant values.

- The heat transfer is mainly carried out in stationary state, so other forms of energy are not taken into account.

3.1. Mass and energy balance

Temperature, mass flow rate and salinity of different objects in the desalination system are listed in Table 1. The equation for the water balance is expressed as:

$$M_a = M_b + M_c \quad (1)$$

where M_a , M_b , M_c represent the mass flow rate of the spray part, steam and concentrated brine, respectively.

The equation for the salt balance is expressed as:

$$M_a X_1 = M_c X_2 \quad (2)$$

where X_1 and X_2 represent the salinity of the spray seawater and concentrated brine, respectively.

The energy balance equation in the falling-film horizontal tube evaporator can be expressed as:

$$C_p [M_c(T_3 - T_1) + M_b(T_2 - T_1)] + rM_b = C_p(T_5 - T_6)M_e \quad (3)$$

Similarly, the energy balance in the condensing fin pipe can be expressed as:

$$C_p(T_8 - T_7)M_f = C_p(T_2 - T_4)M_d + rM_d \quad (4)$$

where r represents water latent heat of vaporization and C_p represent water specific heat capacity.

3.2. Balance of gas phase transition process

Based on supposition (iv), the whole system is hermetic. Only water vapor and non-condensable gases participate in reaction. So Raoult Theorem (Eq. (5)) condition is matched.

$$(p_A^* + p_B^*)V = nRT \quad (5)$$

where p_A^* is the pressure of saturated steam, p_B^* is the pressure of non-condensable gases at the initial time, V and T are the volume and absolute temperature, n is the number of moles of gas; and R is the ideal gas constant. Based on

Raoult Theorem, supposition (ii) and pressure distribution proportion, following equations are acquired.

$$P_A = (1-x)p_A^* \quad (6)$$

$$P_B = p_B^* \quad (7)$$

$$P = P_A + P_B = (1-x)p_A^* + p_B^* \quad (8)$$

$$P_A = y_A P \quad (9)$$

where y_A is the proportion of water vapor, χ is the concentration of solution, P_A is the pressure of water vapor varying with time and P_B is the pressure of non-condensable gases varying with time.

According to Level Rule, the quantity of water vapor can be determined in this phase. Ratio of gas to liquid is ratio of "lever arms" based on Level Rule, shown as Eq. (10).

$$\frac{n_g}{n_l} = \frac{(1-x) - y_A^*}{y_A^* - y_A} \quad (10)$$

where n_g and n_l represent the quantity of gas and liquid, respectively. y_A^* represents the proportion of saturated steam in all gases and is a constant. So, when $1-x = y_A^*$ satisfies, it reaches the balanced point. The balanced point and quantitative analysis are calculated based on systematic parameters.

Vacuum degree in operation process is decreased to -81.2, namely 20.1 kPa. Under 90°C condition, pressure of saturated steam is 70.14 kPa. So the concentration of solution can be calculated.

$$x = 1 - y_A^* = 1 - \frac{p_A^*}{p_A^* + p_B^*} = 1 - \frac{70.14}{70.14 + 20.1} = 0.223 \quad (11)$$

Then the ratio of water vapor to all gases is calculated.

$$y_A = \frac{P_A}{P_A + P_B} = \frac{(1-x)p_A^*}{(1-x)p_A^* + p_B^*} = \frac{(1-0.223) \times 70.14}{(1-0.223) \times 70.14 + 20.1} = 0.731 \quad (12)$$

Table 1
Temperature, mass flow rate and salinity of various objects in the desalination system

Object	Temperature (°C)	Mass flow rate (kg/h)	Salinity (%)
Spray seawater	T_1	M_a	X_1
Steam	T_2	M_b	0
Strong brine	T_3	M_c	X_2
Freshwater	T_4	M_d	0
Heating water input	T_5		0
Heating water output	T_6	M_e	0
Cooling water input	T_7		0
Cooling water output	T_8	M_f	0

According to Eqs. (11) and (12), after evaporation, the concentration of evaporated liquid is 22.3% and the ratio of steam to all gases is 73.1%.

3.3. Calculation of the cross-section heat transfer coefficient

The coefficient of heat transfer in the process of heat exchange can be obtained from the horizontal pipe parameters and seawater spray flow.

3.3.1. Calculation of heat transfer coefficient in horizontal tube part

Forced convection is a mechanism, or type of transport in which fluid motion is generated by an external source. In the horizontal tube, hot water flow is motivated by the pump, so that the heat transfer in the tube is considered as forced convection. The heat transfer coefficient h can be determined by the following Eq. (13) [23]:

$$h = \frac{\text{Nu}_f \lambda}{d_e} \quad (13)$$

where Nu is the Nusselt number of the fluid, d_e is the equivalent diameter of the pipe, and λ is the fluid heat conductivity. The subscript f indicates that the parameter is determined by the average temperature of the fluid, and the subscript W indicates that the parameter is determined by the average wall temperature.

The flow of high-temperature water in the tube is turbulent, and its Nusselt number Nu is calculated as follows [23]:

$$\text{Nu}_f = 0.023 \text{Re}_f^{0.8} \text{Pr}_f^{0.4} \quad (14)$$

$$\text{Re}_f = \frac{u_f d}{\nu_f} \quad (15)$$

$$\text{Pr}_f = \frac{v_f}{a} = \frac{\eta_f c_p}{\lambda_f} \quad (16)$$

Re is the Reynolds number of the fluid, Pr is the Planck number. u_f is the flow velocity determined by the fluid average temperature, d is the pipe inner diameter, ν_f is the kinematic viscosity of fluid determined by the fluid average temperature, a is thermal diffusivity, η_f is the viscosity of fluid determined by the fluid average temperature, c_p is specific heat capacity with certain pressure, λ_f is the fluid heat conductivity determined by the fluid average temperature. Correction is taken into consideration, so Eq. (17) can be acquired.

$$\text{Nu}_f = 0.023 \text{Re}_f^{0.8} \text{Pr}_f^{0.4} \varepsilon_i \varepsilon_l \varepsilon_R \quad (17)$$

where ε_i is the entrance effect correction factor which considers how inlet may influence heat transfer coefficient h .

For short tubes whose $l/d < 60$, $\varepsilon_i = 1 + \left(\frac{d}{l}\right)^{0.7}$. The length and

inner diameter of straight part of the horizontal tube are 200 and 8 mm, respectively, so in Eq. (17), $\varepsilon_i = 1 + \left(\frac{8}{200}\right)^{0.7} = 1.105$.

ε_l is the temperature correction factor considering the effect of temperature distribution in boundary layer on heat transfer coefficient h . Here, the working medium is heated liquid, so $\varepsilon_l = \left(\frac{\eta_f}{\eta_w}\right)^{0.11}$. η is the viscosity of fluid and the meaning of subscription has been illustrated before. ε_R is curving tube effect correction factor. As for the horizontal tube evaporator, the tubes are arranged in several layers and the straight part is far longer than curving part, so $\varepsilon_R = 1$. Therefore, Nusselt number can be calculated by Eq. (18).

$$\text{Nu}_f = 0.025 \text{Re}_f^{0.8} \text{Pr}_f^{0.4} \left(\frac{\eta_f}{\eta_w}\right)^{1.1} \quad (18)$$

The equation is suitable under the condition that $0.7 \leq \text{Pr}_f \leq 120$, $10^4 \leq \text{Re}_f \leq 1.2 \times 10^5$, $\frac{l}{d} < 60$.

3.3.2. Principle of heat transfer outside tube in evaporation process

The heat transfer process outside the tube in the evaporation section can be regarded as the phase transition process of the water film on the surface of the circular tube. Pressure in the evaporator is 0.6 standard atmospheric pressure, therefore, surface phase transition heat transfer coefficient can be calculated by Eq. (19) [23] which is suitable for the condition that pressure is in the range of $(0.2 \sim 101) \times 10^5 \text{Pa}$.

$$h = 0.1448 \Delta t^{2.33} p^{0.5} = 0.56 q^{0.7} p^{0.15} \quad (19)$$

where $\Delta t = (t_w - t_s)^\circ\text{C}$ is superheat degree of tube wall and t_w is tube wall temperature, t_s is steam saturation temperature under corresponding pressure, q (W/m^2) is wall heat flux, p (Pa) is water spoiling absolute pressure. The equation is suitable under the condition that the influence of the tubes between each other is ignored.

3.4. Calculation of the heat transfer coefficient of the condensing section

The type of fin is rectangular cross-section straight fin. The fin efficiency η_{fin} can be computed by the following formula [24]:

$$\eta_{\text{fin}} = \frac{\tanh(mH')}{mH'} \quad (20)$$

$$H' = H_f + \frac{\delta_f}{2} \quad (21)$$

where H_f is the fin height (m); δ_f is the fin thickness (m) shown in Fig. 7; m is a coefficient that can be calculated by Eq. (22):

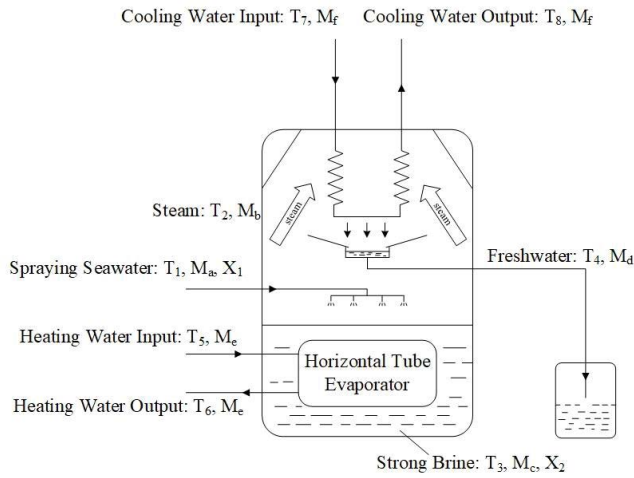


Fig. 7. Input and output of mass and energy in the desalination system.

$$m = \sqrt{\frac{2h_0}{\lambda_{fin}\delta_f}} \quad (22)$$

In Eq. (22), h_0 is the fin surface thermal conductance with water vapor, $W/(m^2 K)$; P is the fin cross-sectional perimeter along the fin height direction, m ; λ_{fin} is the fin material thermal conductivity, $W/(m K)$.

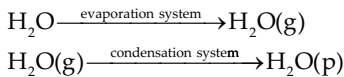
The total heat transfer coefficient of fin tube based on the total surface area A_0 of fin side can be calculated by the following formula [24]:

$$k_f = \frac{1}{\frac{A_0}{h_i A_i} + \frac{\delta A_0}{\lambda_w A_i} + \frac{1}{h_0 \eta_0}} \quad (23)$$

where η_0 is the overall fin surface efficiency, $\eta_0 = (A_1 + \eta_f \times A_2)/A_0$ and $A_0 = A_1 + A_2$. A_1 is plain area between fins, m^2 ; A_2 is the fin surface area, m^2 ; A_i is the refrigerant-side heat exchange area, m^2 . h_i is the surface conductance with cooling water in the condenser, $W/(m^2 K)$; λ_w is the thermal conductivity of condenser wall, $W/(m K)$; δ is the condensing tube wall thickness, m .

3.5. Theoretical analysis of physical state transition process

In one-way irreversible process:



where H_2O presents seawater, $H_2O(g)$ presents water vapor, $H_2O(p)$ presents pure water. H_2O , $H_2O(g)$, $H_2O(p)$ are presented with A , B , C , respectively.

The brackets indicate the amount of substance in the seawater desalination system and its unit is mol. For example, $[A]$ means the amount of substance of seawater in the system. Water is input constantly and remains at $[A]_0$, namely $[A] \sim N([A]_0, \sigma)$. $[A]$ satisfies a normal distribution in which mathematic expectation is $[A]_0$ and variance is σ^2 .

$l(t)$ represents pure water output rate and the unit is mol/L , which refers to the freshwater flowing outside and separated from the system. Based on reaction rates in kinetics, the theoretical process is as follows:

$$\frac{d[A]}{dt} = [A]_0 \quad (24)$$

$$\frac{d[B]}{dt} = k_1[A] - k_2[B] \quad (25)$$

$$\frac{d[C]}{dt} = k_2[B] + l(t) \quad (26)$$

Then time-dependent differential equation is acquired.

$$\begin{cases} [B] = -\frac{k_1[A]_0}{k_2} e^{-k_2 t} + \frac{k_1[A]_0}{k_2} \\ [C] = \frac{k_1[A]_0}{k_2} e^{-k_2 t} + k_1[A]_0 t - \frac{k_1[A]_0}{k_2} \end{cases} \quad (27)$$

Both k_1 and k_2 are constants and their units both are s^{-1} . Based on the properties of analytical solution function, total seawater in the device keeps constant. As the evolution with this system ($t \rightarrow \infty$), steam tends to be constant at $\frac{k_1[A]_0}{k_2}$ ($[B] \rightarrow \frac{k_1[A]_0}{k_2}$) and pure water will output constantly at the value of $k_1[A]_0$ ($\frac{d[C]}{dt} \rightarrow k_1[A]_0$).

3.6. Water desalination system stability

To take the derivative of Eq. (26) and then combine with Eq. (25), in addition, from Eq. (26) it is known that

$$k_2[B] = \frac{d[C]}{dt} - l(t), \text{ so Eq. (28) is acquired.}$$

$$\left(\frac{d^2}{dt^2} + k_2 \frac{d}{dt} \right) [C] = k_1 k_2 [A] + p(t) \quad (28)$$

In Eq. (28), there is relationship of $p(t) = \left(k_2 + \frac{d}{dt} \right) l(t)$. With Laplace transform, Eq. (28), is converted to Eq. (29).

$$C(s) = \frac{1}{s^2 + k_2 s} (k_1 k_2 A(s) + P(s)) \quad (29)$$

Considering the actual meaning of $P(s)$ is a loop feedback, Eq. (30) can be obtained.

$$p(t) = \left(l_1 + l_2 \frac{d}{dt} \right) [C] \quad (30)$$

l_1 and l_2 are constants. Then the analytical expression of output Eq. (31) is acquired by the gain in the forward and loop gain function of feedback system.

$$C(s) = \frac{k_1 k_2}{s^2 + (k_2 + l_2)s + l_1} A(s) \tag{31}$$

The condition for system stability is that the situation which makes the system break down does not happen. In time domain, the stability condition is that its square is integrable. In addition, in frequency domain after Laplace transform, the stability condition equivalent to the positive number domain is convergence, which means zero point is in negative number domain. The mathematical expression is as follows:

$$\begin{cases} \Delta > 0 \\ \frac{-l_2 - k_2 + \sqrt{\Delta}}{2} < 0 \end{cases} \tag{32}$$

where $\Delta = (l_2 + k_2)^2 - 4l_1$. The most optimum stable domain is acquired.

$$l_2 = 0, 0 < l_1 < \frac{\sqrt{k_2}}{2} \tag{33}$$

This means when production is in the range of 0 to $\frac{\sqrt{k_2}}{2}$, the system is stable. When the system is impacted by outside impacts, it can recover to stable state and continue the work very soon.

So far, working process in the desalination device and system performance analysis are finished. In addition, the theoretical values of corresponding production (freshwater, steam) are obtained and the stable working condition for the system is decided finally. In the following part, experimental fitting and analysis will be discussed.

4. Experimental results and analysis

The experiment is conducted indoors, with ambient temperature from 20°C to 25°C and an ambient relative humidity of 50%–70%. The effects of temperature and flow on water yield are measured. Both transient and steady-state water production performances of the small desalination plant are also obtained. Variable-controlling approach is adopted in our experiments.

4.1. Transient performance analysis of the device

Achieving a stable state in a relatively short period of time is important to improve desalination efficiency. In the transient performance experiment of the system, the water temperature of the horizontal-tube falling-film evaporator is set at 80°C, the internal and external fin condenser water temperature is set at 20°C, and the spray flow rate is set at 0.4 L/min. The salt water is placed at the tank bottom, and water yield is recorded every 5 min after the device startup. The corresponding temperature values are measured using a thermocouple and read by a computer.

In the 60 min after system startup, the relationship between total water yield with time is shown in Fig. 8 and

the relationship between water yield every 5 min and time is shown Fig. 9. The operating parameters of the system are as follows: heating water flow of the horizontal-tube falling-film evaporator is 3 ± 0.25 L/min; heating water temperature is $80^\circ\text{C} \pm 2.5^\circ\text{C}$; internal and external fin condenser cold water flow is 8 ± 0.5 L/min, cold water temperature is $20^\circ\text{C} \pm 1^\circ\text{C}$; and circulation spray pump flow = 0.4 ± 0.1 L/min. Fig. 10 illustrates how the circulating water temperature in the tank changes with the time.

Figs. 8 and 9 show that the cumulative freshwater output increases as time increases. Meanwhile, the water production rate first increases and then decreases. The fresh water yield of the system reaches maximum in approximately 25 min. After that, the rate of freshwater production decreases for the reason that system vacuum is reducing. Before the system operates, the vacuum environment is provided by a vacuum pump and the vacuum is no longer complemented during system operation. After the system vacuum level becomes stable, the water production rate of the system becomes basically stable at approximately 40 min. When the

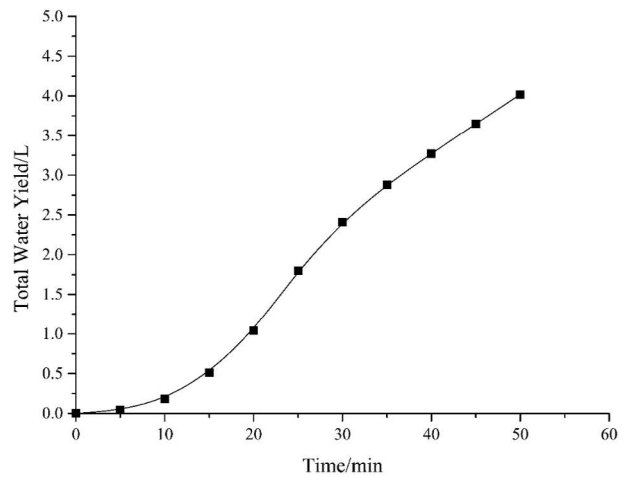


Fig. 8. Variations in total water yield after the system starts up.

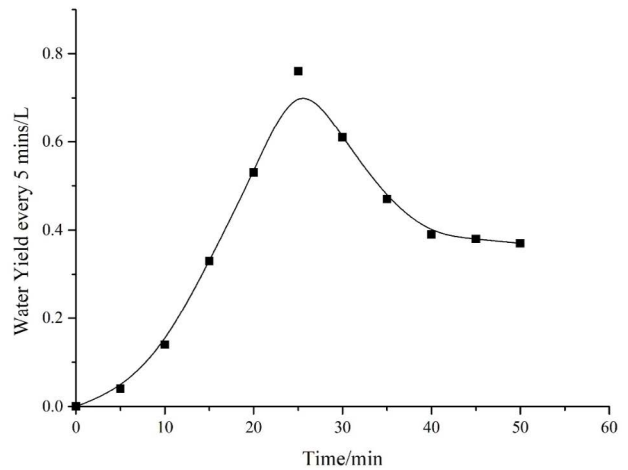


Fig. 9. Variations in water yield every 5 min.

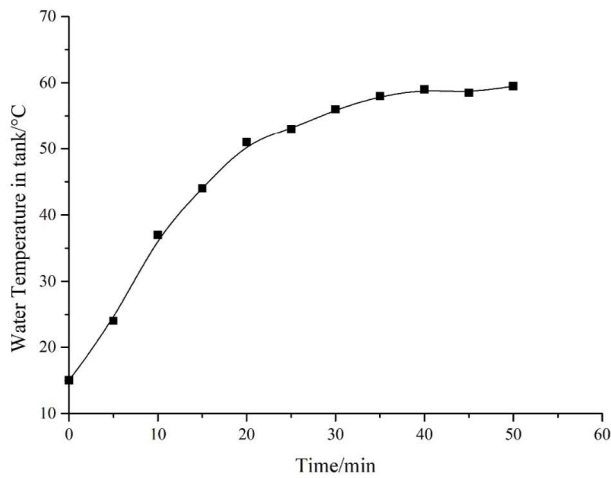


Fig. 10. Variations of the water temperature in the tank after the system starts up.

system is running, the system temperature generally rises and is basically stable at approximately 25 min.

4.2. Steady-state performance analysis of the device

The steady-state performance of the device is an important index to measure the stability and reliability of the device. In steady-state condition, a high water yield indicates a good system performance. Therefore, the steady-state performance of the system is meaningful to be tested.

In this part, unless the parameter is set as the variable to be researched, the initial parameters are set as follows: heating water flow of the horizontal-tube falling-film evaporator is 3 ± 0.25 L/min; heating water temperature is $80^\circ\text{C} \pm 2.5^\circ\text{C}$; internal and external fin condenser cold water flow is 8 ± 0.5 L/min, cold water temperature is $20^\circ\text{C} \pm 1^\circ\text{C}$; and circulation spray pump flow = 0.4 ± 0.1 L/min.

4.2.1. Steady-state water production performance of the device

Under the condition of stable operation (heat balance state), when the heating water temperature is $80^\circ\text{C} \pm 2.5^\circ\text{C}$, the effects of different hot water flows on the water yield every 10 min and on the temperature difference between inlet and outlet of evaporators are shown in Fig. 11.

Fig. 11 demonstrates that, as the hot water flow increases, the water production rate also increases. In addition, production rate of 4 L/min is more than 1.5 times than that of 1.5 L/min. However, larger flow also leads to higher power consumption. An evaluation index for the effect of flow on water yield will be presented in the next section. The effect of hot water temperature on freshwater yield under fixed horizontal pipe flow is shown in Fig. 12.

Fig. 12 illustrates that a higher heating water temperature in the evaporator results in higher production rate of fresh water. Production rate under the temperature of 80°C is more than 1.5 times higher than that of 70°C . The system performs better at producing water at higher temperature. The efficiency reaches optimum when heating water temperature is controlled in the range of 75°C – 85°C .

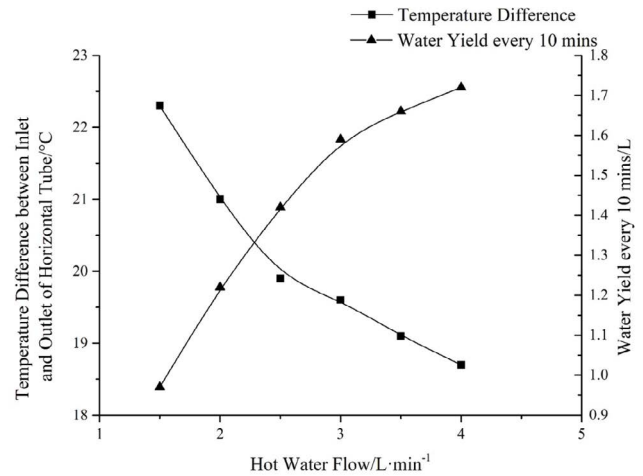


Fig. 11. Effect of hot water flow in horizontal tubes on water output every 10 min and temperature differences between inlet and outlet of horizontal tubes.

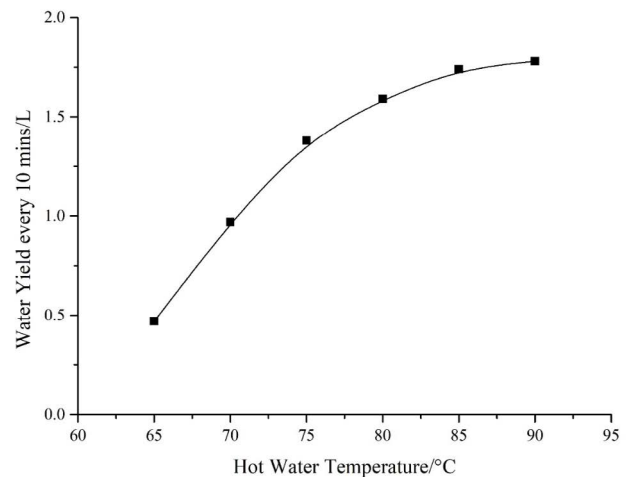


Fig. 12. Variation in water yield every 10 min as hot water temperature changes.

Under the condition of stable operation, namely heat balance state, and a cooling water temperature of 20°C , the effects of different cold water flows on the water yield every 10 min is shown in Fig. 13.

Fig. 13 shows that, as the flow increases, the water production rate also increases. In addition, production rate of 10 L/min cold water flow is as twice as that of 5 L/min cold water flow. An evaluation index for the effect of flow on water yield is proposed in the next section.

4.2.2. Steady-state performance ratio of the device

A thermodynamic performance evaluation index based on the first law of thermodynamics for the thermal seawater desalination device is adopted. The thermodynamic performance index refers to the heat consumption of per unit freshwater production q . The thermal system evaluation index determined by the first law of thermodynamics varies with

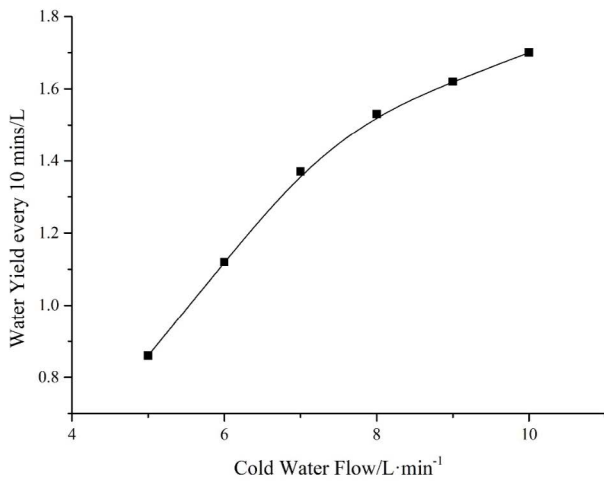


Fig. 13. Variation in cumulative water yield with the change in condenser pipe flow.

different distillation desalination principles. For a single-effect solar desalination device, the system heat source comes from hot water working fluid heated by solar power. The thermal performance index is expressed by the heat consumption rate q per unit freshwater output.

$$q = \frac{Q_b}{M_d} \tag{34}$$

where Q_b refers to heat released by hot water working fluid (kJ/h) and M_d refers to freshwater yield (t/h). The relationship between hot water flow and heat consumption rate q in this desalination system is shown as Fig. 14.

The diagram shows that the heat consumption rate decreases with the increment of hot water flow in the horizontal tube. The analyzed reason is that the higher hot water flow rate causes higher thermal energy input and higher flow velocity. The former leads to better heat transfer

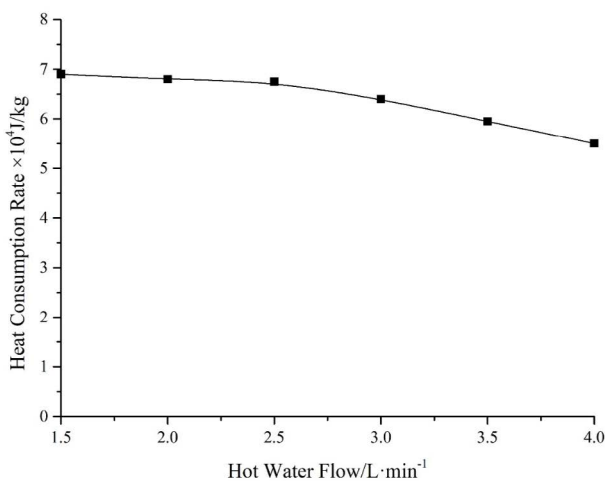


Fig. 14. Variation in performance ratio with the change in hot water flow.

efficiency but the latter counters. The positive influence of higher energy input exceeds the negative influence of higher flow velocity. Therefore, energy consumption of freshwater production per unit reduces. However, this parameter of energy consumption can only compare the amount of freshwater produced by the same thermal energy. In fact, the energy required for the system is not only the heat source but also the pump and other devices. As a result, performance ratio (PR) is appropriate to be chosen as the comprehensive performance index of the system instead of heat consumption rate.

The performance ratio PR [25] of the seawater desalination device is an important index for the system performance assessment. A large performance ratio shows a superior system performance. According to the input–output relationship, the steady-state performance ratio of the device is given as the following form:

$$PR = \frac{M_e h_{fg}}{Q + P_s \Delta t} \tag{35}$$

where M_e (kg/h) is the water yield of the seawater desalination system; h_{fg} (kJ/kg) is the latent heat of water vaporization, approximately $h_{fg} = 2,350$ kJ/kg; Q (kJ) is the total input thermal energy; P_s (kW) is the mechanical power consumed by the seawater desalination system; Δt (s) is the operation time.

When the temperature of heating water is 80°C, internal and external fin condenser cold water flow is 8 ± 0.5 L/min, cold water temperature is $20^\circ\text{C} \pm 1^\circ\text{C}$ and circulation spray pump flow = 0.4 ± 0.1 L/min, the relationship between different hot water flows and performance ratio is illustrated in Fig. 15.

Fig. 15 shows that the performance ratio increases first and then decreases with the increment of hot water flow. The flow rate of hot water should be set in the best range of 2–3 L/min by the comprehensive consideration of the device energy consumption and water production.

The flow coefficient of the seawater desalination system is an important reference coefficient for designing principal components. The flows of other components can be

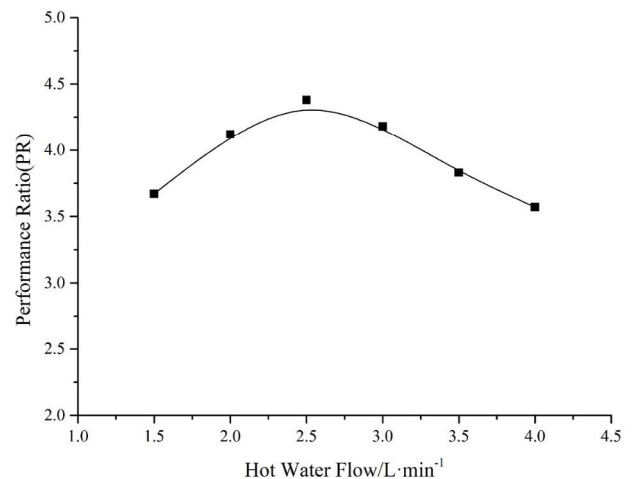


Fig. 15. Effect of hot water flow on performance ratio PR.

determined based on one set flow. The flow coefficient is given by the following formula:

$$K = \frac{Q_p}{Q_a} \quad (36)$$

where K is the flow coefficient of the seawater desalination system; Q_p (L/min) is a set flow; Q_a (L/min) is the flow of a component selected according to the set flow.

In this study, spraying flow is constantly set as 0.4 L/min, therefore according to Fig. 15, the flow coefficient of the horizontal pipe (the ratio of spraying flow to horizontal pipe flow) is the best in the range of 0.15–0.2.

When the cooling water temperature is set at 20°C, the relationship between the different condensing water flow rates and the performance ratio is shown in Fig. 16.

Fig. 16 shows that with the increment of the cold water flow rate, the performance ratio increases first and then gradually decreases. The flow rate of cold water should be set in the range of 7–9 L/min in comprehensive consideration of the device energy consumption and water production. Under the condition that spraying flow has been set as 0.4 L/min, the condensing water flow coefficient (ratio of spraying flow to condensing fin tube flow) is optimal in the range of 0.045–0.055.

The average salinity of produced water is approximately 96 mg/kg. The World Health Organization standard for potable water is 500 mg/kg [1]. Therefore, water produced by this desalination system satisfies the potable water standard. Since the set salinity of discharged brine is 100 g/kg, its salinity is more than 1,000 times as the produced water's. The experimental results are compared with similar researches. Feng et al. [26] designed and manufactured a plate-type distillation desalination device based on the thermodynamics principle of PHE. They pointed out hot water inlet temperature and flow are important factors influencing distillation freshwater production rate. Production rate linearly increases as temperature and hot water flow rise, respectively. These results are identical to ours (shown in Figs. 11 and 12). In addition, they discovered there was an optimal middle value of feed water flow. However, our team conducted more

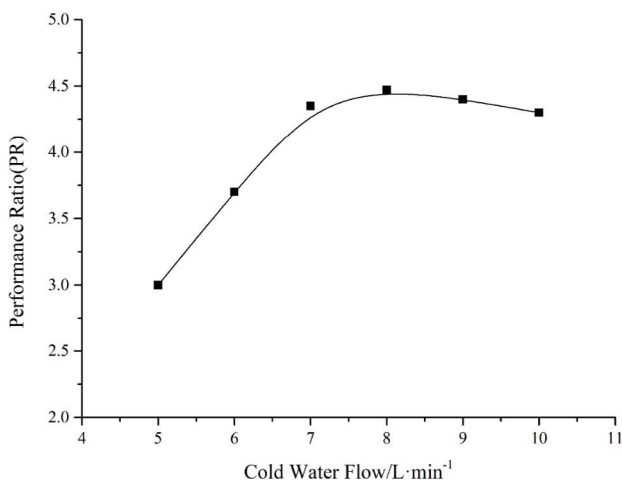


Fig. 16. Effect of cold water flow on performance ratio PR.

experiments about transient state performance and explored how cold water influencing production rate in steady state. Luca et al. [27] designed and tested a single-effect thermal desalination plant in order to recover the thermal power output from a 1 kWe Stirling engine. The maximum fresh water production can be higher than 7 L/h and the plant average efficiency was about 1.3 L/kWh of energy input with minimum and maximum values equal to 1.16 and 1.42 L/kWh. Moreover, they explored the effect of evaporator tank saturation temperature, temperature difference between the heating fluid and the salt water, heating fluid flow rate on thermal power input, fresh water production, heat transfer coefficient and plant efficiency, respectively. The influence of hot flow rate is in good agreement with our study but they also ignored the effect of cold water flow rate. More work relevant to energy consumption of freshwater per liter and heat transfer coefficient of each component is planned to carry out in order to better evaluate the miniature low-temperature solar seawater desalination plant.

5. Conclusion

The study evaluates the transient and steady-state performance of a lightweight low-temperature distillation seawater desalination device and obtains the following experimental conclusions:

- The system has a high water production rate under steady-state conditions. When the temperature of heating water is set between 75°C–85°C, the steady-state water production rate can reach above 8 L/h.
- The device adapts several methods such as horizontal-tube falling-film evaporation, atomization spraying, internal and external fin tube condensation and so on to intensify heat transfer and improve the freshwater output efficiency. The device starts up fast and fresh water outputs within 1 min operation after startup. At approximately 25 min, fresh water producing rate peaks. The water production rate in the system is stable in approximately 40 min. When the entire device is running, the system temperature generally increases and is stabilized within 25 min. The steady-state performance ratio of the device can reach approximately 4.
- To comprehensively evaluate both water producing rate and energy consumption of the device, the desalination system performance can be evaluated by the steady performance ratio. The operation state is optimal when the horizontal tube flow rate is in the range of 2–3 L/min and the flow coefficient is in the range of 0.15–0.2. Similarly, the operation state reaches best when the cold water flow rate in the inner and outer fin condenser pipes is in the range of 7–9 L/min and the flow coefficient is in the range of 0.045–0.055.

In the future, our team plan to combine the vacuum chamber technology with fin condenser and replace film-falling horizontal tube with plate heat exchanger to further improve heat transfer efficiency. In addition, we consider utilizing venturi tube instead of vacuum pump to achieve the goal of keeping desalination system vacuum. With these improvements, we aim at further developing heat transfer efficiency in the desalination system.

Acknowledgements

This study was supported by: Natural Science Foundation of Shandong Province (Grant No. ZR2017BEE012); Focus on research and development plan in Shandong Province (Grant No. 2018GGX104011).

Symbols

δ_f	—	Fin thickness
S_f	—	Fin spacing
H_f	—	Fin height
d_i	—	Fin tube inner minimum diameter
d_f	—	Fin tube outer maximum diameter
r	—	Water latent heat of vaporization
C_p	—	Water specific heat capacity
T_1	—	Spray seawater temperature
T_2	—	Steam temperature in the tank
T_3	—	Strong brine temperature
T_4	—	Freshwater temperature
T_5	—	Heating water input temperature
T_6	—	Heating water output temperature
T_7	—	Cooling water input temperature
T_8	—	Cooling water output temperature
M_a	—	Spray seawater mass flow rate
M_b	—	Steam mass flow rate
M_c	—	Strong brine mass flow rate
M_d	—	Freshwater mass flow rate
M_e	—	Heating water mass flow rate
M_f	—	Cooling water mass flow rate
X_1	—	Salinity of spray seawater
X_2	—	Salinity of strong brine
p_A^*	—	Pressure of saturated steam
p_B^*	—	Pressure of non-condensable gases at the initial time
V	—	Volume of gases in main tank
T	—	Temperature of gases in main tank
n	—	Number of moles of gases in main tank
R	—	Ideal gas constant
y_A	—	Proportion of water vapor in main tank
x	—	Concentration of solution in main tank
P_A	—	Pressure of water vapor varying with time in main tank
P_B	—	Pressure of non-condensable gas varying with time in main tank
n_g	—	Quantity of gas in main tank
n_l	—	Quantity of liquid in main tank
y_A^*	—	Proportion of saturated steam in main tank
h	—	Heat transfer coefficient
Nu	—	Nusselt number of fluid
d_e	—	Equivalent diameter of pipe
λ	—	Fluid heat conductivity
λ_f	—	Fluid heat conductivity determined by the fluid average temperature
Re_f	—	Reynolds number determined by fluid average temperature
u_f	—	Flow velocity determined by the fluid average temperature
d	—	Pipe inner diameter
ν_f	—	Kinematic viscosity of fluid determined by the fluid average temperature

a	—	Thermal diffusivity
η_f	—	Viscosity of fluid determined by the fluid average temperature
η_w	—	Viscosity of fluid determined by the average wall temperature
c_p	—	Specific heat capacity with certain pressure
ε_l	—	Entrance effect correction factor
ε_t	—	Temperature correction factor
ε_R	—	Curving tube effect correction factor
t_w	—	Tube wall temperature
t_s	—	Steam saturation temperature under corresponding pressure
q	—	Wall heat flux
p	—	Water spoiling absolute pressure
η_{in}^f	—	Fin efficiency
m	—	Coefficient for fin calculation
h_0	—	Fin surface thermal conductance with water vapor
P	—	Fin cross-sectional perimeter along the fin height direction
λ_{fin}	—	Fin material thermal conductivity
η_o	—	Overall fin surface efficiency
A_1	—	Plain area between fins
A_2	—	Fin surface area
A_i	—	Refrigerant-side heat exchange area
h_i	—	Surface conductance with cooling water in the condenser
λ_w	—	Thermal conductivity of condenser wall
δ	—	Condensing tube wall thickness
A	—	Seawater
B	—	Water vapor
C	—	Pure water
k_1	—	Constant
k_2	—	Constant
l_1	—	Constant
l_2	—	Constant

References

- [1] Q. Chen, M. Kum Ja, Y. Li, K.J. Chua, Evaluation of a solar-powered spray-assisted low-temperature desalination technology, *Appl. Energy*, 211 (2018) 997–1008.
- [2] C. Li, Y. Goswami, E. Stefanakos, Solar assisted sea water desalination: a review, *Renew. Sustain. Energy Rev.*, 19 (2013) 136–163.
- [3] Kalogirou, A. Soteris, Seawater desalination using renewable energy sources, *Progr. Energy Combust. Sci.*, 31 (2005) 242–281.
- [4] H. Chung, J. Hyomin, J. Kwang-Woon, C. Soon-Ho, Improved productivity of the MSF (multi-stage Flashing) desalination plant by increasing the TBT (top brine temperature), *Energy*, 107 (2016) 683–692.
- [5] A.D. Khawajia, K. Kutubkhanah, J.-M. Wie, Advances in seawater desalination technologies, *Desalination*, 221 (2008) 47–69.
- [6] G. Micale, L. Rizzuti, A. Cipollina, *Seawater Desalination: Conventional and Renewable Energy Processes*, Springer Berlin Heidelberg, Berlin, Heidelberg, 2009.
- [7] A. Pérez-González, A.M. Urriaga, R. Ibáñez, I. Ortiz, Review-State of the art and review on the treatment technologies of water reverse osmosis concentrates, *Water Res.*, 46 (2012) 267–283.
- [8] N. Manjula, K. Dinesh, Water desalination and challenges: the Middle East perspective: a review, *Desal. Wat. Treat.*, 51 (2013) 2030–2040.
- [9] C. Fritzmann, J. Löwenberg, T. Wintgens, T. Melin, State-of-the-art of reverse osmosis desalination, *Desalination*, 216 (2007) 1–76.

- [10] Choi, Soon-Ho, Thermal type seawater desalination with barometric vacuum and solar energy, *Energy*, 141 (2017) 1332–1349.
- [11] X.L. Wang, N. Kim Choon, Experimental investigation of an adsorption desalination plant using low-temperature waste heat, *Appl. Thermal Eng.*, 25 (2005) 2780–2789.
- [12] K. Gustavo, L. Fredi, Low-temperature distillation processes in single-and dual-purpose plants [J], *Desalination*, 136 (2001) 189–197.
- [13] D.F. Zhao, J.L. Xue, S. Li, H. Sun, Q.D. Zhang, Theoretical analyses of thermal and economical aspects of multi-effect distillation desalination dealing with high-salinity wastewater, *Desalination*, 273 (2011) 292–298.
- [14] G.N. Tiwari, L. Sahota, Review on the energy and economic efficiencies of passive and active solar distillation systems, *Desalination*, 401 (2017) 151–179.
- [15] G.N. Tiwari, J.K. Yadav, D.B. Singh, I.M. Al-Helalb, A.M. Abdel-Ghanyb, Exergoeconomic and enviroeconomic analyses of partially covered photovoltaic flat plate collector active solar distillation system, *Desalination*, 367 (2015) 186–196.
- [16] K.S. Reddy, H. Sharon, Energy-environment-economic investigations on evacuated active multiple stage series flow solar distillation unit for potable water production, *Energy Convers. Manage.*, 151 (2017) 259–285.
- [17] M. Chandrashekhara, Y. Avadhes, Water desalination system using solar heat: a review, *Renew. Sustain. Energy Rev.*, 67 (2017) 1308–1330.
- [18] A.A. El-Sebaei, E. El-Bialy, Advanced designs of solar desalination systems: a review, *Renew. Sustain. Energy Rev.*, 49 (2015) 1198–1212.
- [19] Balage Don Lak Srikantha, Design, Development and Testing of an Active Solar Vacuum Water Distiller, Master Thesis, Chongqing University, Chongqing, China, 2014.
- [20] P.K. Ithape, S.B. Barve, A.R. Nadgire, Climatic and design parameters effects on the productivity of solar stills: a review, *Int. J. Current Eng. Scient. Res.*, 4 (2017) 17–23.
- [21] R.S. Hansen, K.K. Murugavel, Enhancement of integrated solar still using different new absorber configurations: an experimental approach, *Desalination*, 422 (2017) 59–67.
- [22] M. Siddique, N. Turkmen, O.M. Al-Rabghi, E. Shabana, M.H. Albeirutty, Small-scale low pressure ‘single effect distillation’ and ‘single stage flash’ solar driven barometric desalination units: a comparative analysis, *Desalination*, 444 (2018) 53–62.
- [23] X.X. Zhang, G.F. Li, L. Shi, Thermal Engineering Foundation, 2nd edn., Higher Education Press, Beijing, China, 2006.
- [24] S.M. Yang, W.C. Tao, Heat Transfer, 3rd edn., Higher Education Press, Beijing 1998.
- [25] Z.Q. Chen, H.F. Zheng, Z.C. Ma, Z.L. Li, K.Y. He, Study on the optimal parameters for the solar heating system for a low-temperature multi-effect solar desalination unit, *Acta Energiæ Solaris Sinica*, 29 (2008) 672–676.
- [26] D.D. Feng, F.M. Zhang, C.J. Su, S.Q. Chen, W.J. Kuang, An experimental study on thermal performance of a single effect distillation desalination device, *J. Integration Technol.*, 6 (2017) 82–86.
- [27] C. Luca, S. Andrea, R. Massimiliano, C. Flavio, C. Gabriele, Design and test of a single effect thermal desalination plant using waste heat from m-CHP Units, *Appl. Thermal Eng.*, 82 (2015) 18–29.